Visible Emission from ZnO Doped with Rare-Earth Ions

W.M. JADWISIENCZAK, H.J. LOZYKOWSKI, A. XU, and B. PATEL

School of Electrical Engineering & Computer Science, Ohio University, Athens, OH 45701-2979

We report the results of a cathodoluminescence (CL) and photoluminescence (PL) study of ZnO-bulk single crystals and epilayer thin-film samples grown on a sapphire (0001) substrate and doped by implantation with rare-earth ions (RE^{3+}): Pr^{3+}, Dy^{3+}, Ho^{3+}, Er^{3+}, Tm^{3+} (bulk crystals, co-doped with Li), Sm^{3+}, Dy^{3+}, and Er^{3+} (epilayers). The PL and PL excitation (PLE) spectra of polycrystalline ZnO doped with RE^{3+} ions (Nd^{3+}, Dy^{3+}, Er^{3+}, and Tm^{3+}) and co-doped with Li^+, Cl^-, and N^- ions have also been studied.

Key words: Luminescence, rare-earth ions, doping, wide bandgap semiconductor, ZnO

INTRODUCTION

The ZnO (wurtzite) is a wide bandgap (3.437 eV at 2 K), naturally n-type semiconductor with a large exciton-binding energy of 60 meV that has attracted much recent attention. The recently reported ability to obtain p-type ZnO[1–5] opens up novel possibilities for optoelectronic light-emitting devices, including lasers operating in the near ultraviolet (UV) and blue spectral range. The low-temperature photoluminescence (PL) emission is dominated by the neutral donor-bound exciton (D°,X) complexes[6] and the green band near 2.4 eV.[7] The mechanism of the green emission is not still completely understood. In the literature are several models relating the green luminescence to transitions between energy levels of interstitial Zn or O vacancy to Zn vacancy. The two different shallow donors, acceptor phonon-assisted recombination is the most probable model.[7] The red and yellow low-intensity luminescence from ZnO is also reported, which are related to impurities.[8] The ZnO can be grown as a large-scale, high-quality bulk and thin-film crystals and possesses a potential as a host for rare-earth (RE) ions doping. When excited by proper radiation, hot carriers-impact excitation, or carriers injected in the p-n junction structure, this material has the potential to display luminescence over wavelengths from UV to infrared and can have applications in electroluminescence (EL) and cathodoluminescence (CL) displays and other optoelectronics devices. However, up to now, the research showed that the main obstacle of ZnO host doped with RE ions is relatively poor luminescence from RE centers compared to that from excitonic emission or self-activated (SA) host centers. In the past, most extensively studied was luminescence of trivalent RE^{3+} ions from sintered ZnO-polycrystalline pellets.[9–18] It was found that the addition of various coactivators mainly lithium ions,[10–17] nitrogen,[18] or chlorine[15–17] compounds usually results in an increase of the luminescence intensity of RE^{3+} ions and a decrease of the intrinsic luminescence of the semiconductor host.

In this article, we present results of a spectroscopic study on luminescence of RE^{3+} ions embedded into ZnO bulk and thin-film single-crystal semiconductor hosts. To our knowledge, this is the first report of the visible emission of RE ions Pr^{3+}, Sm^{3+}, Dy^{3+}, Ho^{3+}, and Tm^{3+} incorporated into ZnO single crystal. We also study the sintered polycrystalline-ZnO:RE pellets, co-doped with Li, Cl, and N ions.

EXPERIMENT

The ZnO material used in this investigation was undoped 10 mm × 10 mm × 0.5-mm melt-grown crystals by Cermet, Inc., Atlanta, GA and ~0.5-μm-thick epilayer thin-film samples grown on a 1-in.-diameter sapphire (0001) substrate by S & R Rubicon, Inc., Chicago IL. The ZnO single crystals and thin-film samples are oriented with the c axis perpendicu-

(Received October 5, 2001; accepted February 28, 2002)

lar to the surface. The ZnO-bulk single crystals and epilayer thin-film samples were doped by implantation with different RE ions at room temperature (and bulk crystals co-implanted with lithium at room temperature). The implantation parameters are summarized in Table I. Each RE ion was implanted at three energies at doses chosen to give an approximately flat implant concentration-depth profile in the ZnO host. The implant concentration-depth profile of Li^+ ions was chosen to overlap with that of the RE ions. The implanting ion beam was inclined at 7° to the normal of the ZnO surface to prevent channeling. The simulated-depth profiles, the projected ranges, and peak concentration were calculated using the Pearson distribution (Table I). In this study, RE-doped ZnO samples were given isochronal thermal-annealing treatments up to 1,150°C in different ambient gasses (or in a vacuum) and were allowed different durations to recover implantation damages and to incorporate the RE ions as the luminescence center. The sintered-polycrystalline materials were RE doped by mixing of 0.6–1% of RE_2O_3 or $RE(NO_3)_3 \times 5H_2O$, with ZnO (99.995% pure, CERAC) and ~1% of Li_2CO_3, pressed under 2 ton/cm^2 into pellets and heated for 2.5–5 h at 1,000–1,180°C in different ambient gasses under atmospheric pressure (Table II). Several ZnO:RE pellets were co-doped with nitrogen or chlorine and fabricated following the procedure described elsewhere.[16–18] The same spectroscopic measurement system as used in an earlier work[19] was employed in this work.

LUMINESCENCE OF BULK AND THIN-FILM ZnO:RE SAMPLES

In general, RE-doped ZnO single-crystal samples show characteristic emission because of 4f-4f transitions after RE ion implantation upon electron-beam excitation. However, some moderate postimplantation annealing treatment enhances the observed emission intensity. The effect of annealing was studied by recording the CL emission spectra after isochronal-annealing treatments performed at successively higher temperature in the range 25–1,100°C. Examples of the evolution of the CL spectra of Sm- and Er-doped ZnO thin films are shown in Figs. 1 and 2. For the ZnO:RE ion-implanted samples, annealing at 150°C (during 20 min) brought up RE emissions approximately two times stronger than recorded for as-implanted (unannealed) ZnO:RE samples. Still fur-

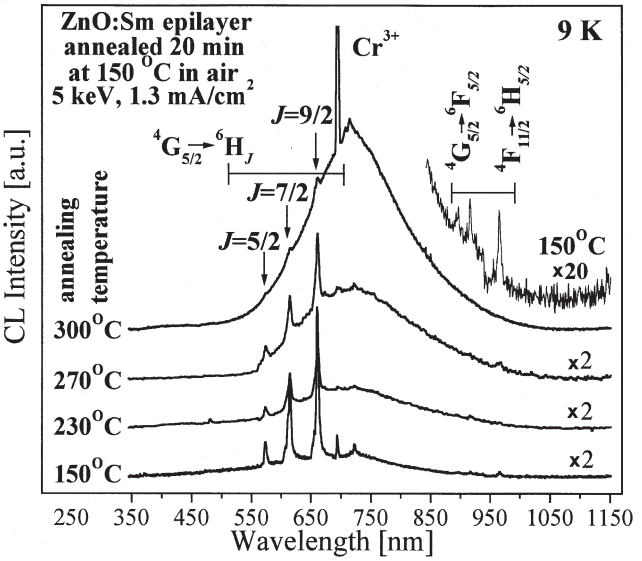

Fig. 1. The effect of annealing on the emission spectra of Sm-doped ZnO thin film measured at 9 K.

Table I. Summary of Implantation Parameters

ZnO Sample	Implanted Ion	Ion Energy (keV)	Ion Dose (cm^{-2})	Projected Range (nm)	Ion Concentration (cm^{-3})
#3 bulk	Pr^{3+}	—	—	~35	3.1×10^{19}
Epilayer	Sm^{3+}	150	1.0×10^{14}	~32	3.5×10^{19}
#3 bulk, epilayer	Dy^{3+}	50	3.0×10^{13}	~31	3.7×10^{19}
#2 bulk	Ho^{3+}	17	1.5×10^{13}	~30	4.1×10^{19}
#2 bulk, epilayer	Er^{3+}	—	—	~28	4.0×10^{19}
#1 bulk	Tm^{3+}	—	—	~28	4.0×10^{19}
#2, 3 bulk	Li^+	7	1.8×10^{14}	~35	3.5×10^{19}

Table II. Fabrication of ZnO:RE-Sintered Pellets

RE Ion Compound	RE Ion Concentration (Mol %)	Co-Activator Compound	Co-Activator Concentration (Mol %)	Firing Conditions
$Nd(NO_3)_3 5H_2O$	0.8	Li_2CO_3	Li^+: 0.8	5 h at 1,180°C in air
Eu_2O_3	0.6	HNO_3	N^-	2.5 h at 400°C in air
Dy_2O_3	0.6	Li_2CO_3	Li^+: 5.78	5 h at 1,000°C in air
$Er(NO_3)_3 5H_2O$	0.6	Li_2CO_3	Li^+: 5.78	5 h at 1,000°C in air
$Tm(NO_3)_3 5H_2O$	0.8	Li_2CO_3	Li^+: 0.8	5 h at 1,180°C in air
$TmCl_3$	1.0	—	Cl^-	2.5 h at 1,100°C in vacuum

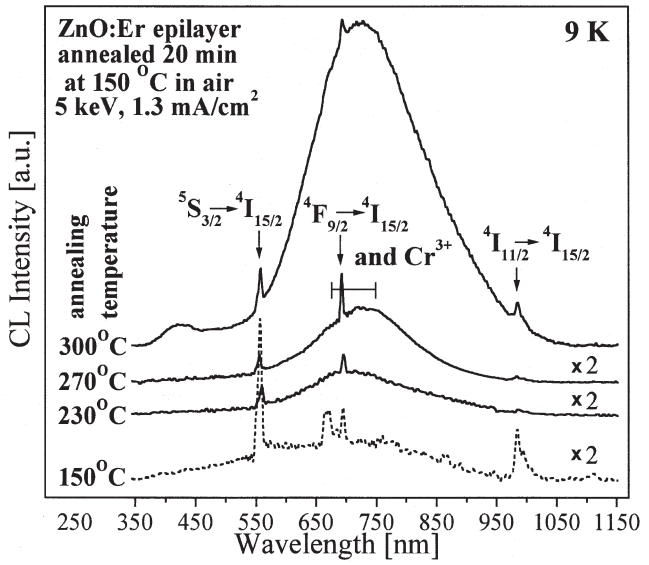

Fig. 2. The effect of annealing on the emission spectra of Er-doped ZnO thin film measured at 9 K.

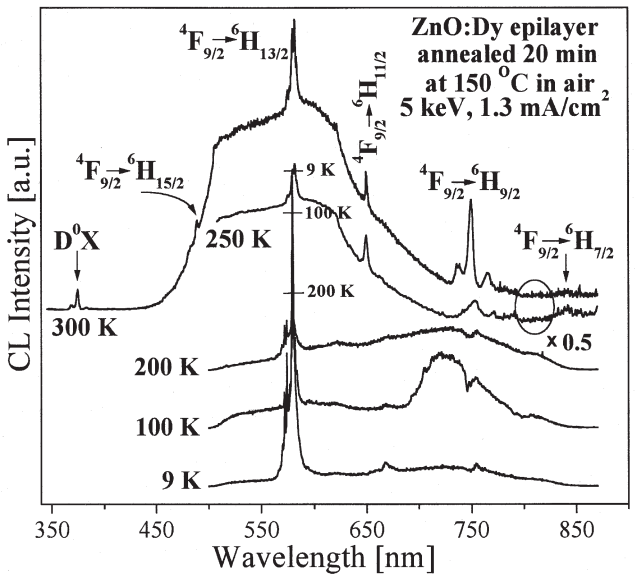

Fig. 3. The CL spectra of Dy-doped ZnO thin-film samples annealed at 150°C in air recorded at different temperature.

ther annealing at temperatures above 150°C revealed that the characteristic sharp-line emission spectra of RE ions became less resolved and gradually disappeared when annealing temperature approaches 300°C. We did not observe the appearance of any new 4f-4f transition lines with rising annealing temperature, unlike other RE-implanted II-VI compounds.[20] It is clearly seen in these figures that ZnO:RE samples annealed at 300°C show a dominant, broad emission band centered at ~720 nm because of SA ZnO-host centers, overlapped with weak RE^{3+} lines. Annealing the samples above 300°C up to 1,100°C (in different ambient and duration times) does not recover RE emissions. The line at 694 nm, which appears in the CL spectra of ZnO:RE thin films, is the Cr^{3+}-emission line originating from the sapphire substrate. A similar observation of Cr^{3+} emission was reported for GaN:RE grown on sapphire.[19]

The CL spectrum of the ZnO:Sm^{3+} epilayer presented in Fig. 1 for a sample annealed at 150°C shows sharp line structures arising from $^4G_{5/2}$ and $^4F_{11/2}$ transitions to the ^6H_J (J = 5/2, 7/2, 9/2) multiplets. The emission spectrum of ZnO:Er^{3+} in Fig. 2 for a sample annealed at 150°C shows several groups of emission lines linked to transitions from $^2S_{3/2}$, $^4F_{9/2}$, and $^4I_{11/2}$ to level $^4I_{15/2}$ of the ground term. In both cases, RE^{3+}-emission lines overlap with the broad band centered at ~650 nm. Figure 3 shows the evolution of the CL spectra for Dy-doped ZnO thin films annealed at 150°C for 20 min in air as a function of temperature in the range of 9–300 K. It is seen that at 9 K the CL spectrum of the ZnO:Dy sample is dominated by $^4F_{9/2} \rightarrow {}^6H_{13/2}$ and small $^4F_{9/2} \rightarrow {}^6H_{9/2}$ transitions overlapped with a weak, very broad band. With increasing sample temperature from 9 K to 200 K, we observed an evolution of CL-emission spectra. The broad band centered at 725 nm appeared together with several sharp depths at 746 nm and 795 nm, respectively, because of the reabsorption processes by RE ions. At still higher temperature (250°C), this band disappeared completely, and a new broad band centered at 560 nm arose. It is seen that at 300 K, new transitions at 490 nm ($^4F_{9/2} \rightarrow {}^6H_{15/2}$) and 842 nm ($^4F_{9/2} \rightarrow {}^6H_{7/2}$) became observable together with the $^4F_{9/2} \rightarrow {}^6H_{9/2}$ transitions, and the host D^oX emission at 375 nm. Figure 4 shows a set of CL (spectrum a–d) and PL (spectrum e) spectra recorded for bulk-ZnO samples implanted with Pr^{3+}, Dy^{3+}, Ho^{3+}, Er^{3+} (co-implanted with Li), and Tm^{3+} ions annealed at 150°C in air and recorded at room temperature. The spectra shown in Fig. 4a–d were recorded at

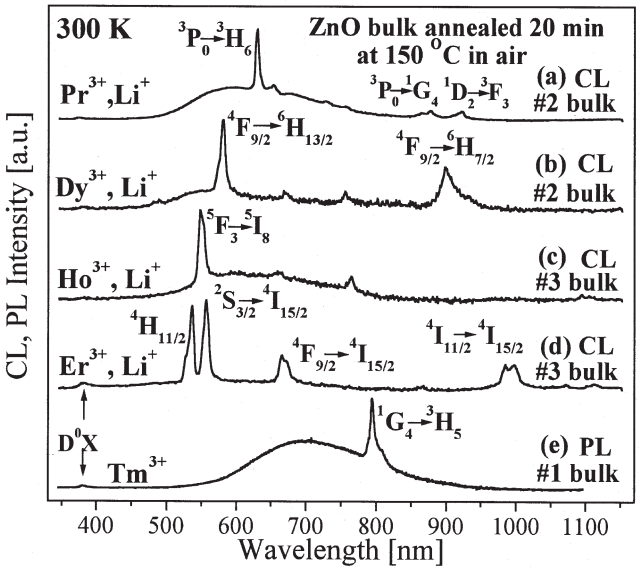

Fig. 4. The room-temperature CL and PL emission spectra of bulk-ZnO single crystals implanted with (a) Pr^{3+}, (b) Dy^{3+}, (c) Ho^{3+}, (d) Er^{3+}, and (e) Tm^{3+} ions, and co-implanted with Li^+ ions (a)–(d). Spectra (a)–(d) were excited by electron beam with an energy of 5 keV and a density of current 1.3 mW/cm^2. Spectrum (e) was excited with 325-nm laser line.

identical conditions using electron-beam excitation with an energy of 5 keV and a beam-current density of 1.3 mA/cm^2. It should be noted that we do not observe clear evidence of influence of Li^+ ions on CL-emission spectra of RE-doped ZnO. All spectra shown in Fig. 4 were normalized to unity at the strongest peak of each spectrum, and we find (a) the emission of ZnO:Pr:Li dominated by the $^3P_0 \rightarrow {}^3H_6$ transition at 630 nm and weak transitions $^3P_0 \rightarrow {}^1G_4$ at 876 nm and $^1D_2 \rightarrow {}^3F_3$ at 920 nm of Pr^{3+}; (b) the spectrum of ZnO:Dy:Li with the strongest peak at 580 nm because of the $^4F_{9/2} \rightarrow {}^3H_{13/2}$ transition of Dy^{3+}; (c) the spectrum of ZnO:Ho:Li with a dominant peak at 547 nm because of the $^5F_3 \rightarrow {}^5I_8$ transition of Ho^{3+}; and (d) the spectrum of ZnO:Er:Li with the two strongest transition lines at 536 nm and 556 nm because of the $^4H_{11/2}$, $^2S_{3/2} \rightarrow {}^4I_{15/2}$ transitions of Er^{3+}, respectively. Figure 4e shows that the PL spectrum of Tm-doped ZnO-bulk crystal, excited by a He-Cd laser (325 nm), and recorded at room temperature is dominated by the $^1G_4 \rightarrow {}^3H_5$ transition of the Tm^{3+} ion at ~800 nm overlapped with a broad band centered at ~700 nm. Excitation of Pr-, Dy-, Ho-, and Er-doped bulk-ZnO:Li samples by the He-Cd laser (325 nm) above the bandgap show only ZnO-host emission. In general, all spectra shown in Fig. 4 exhibit more or less the presence of broad bands because of SA ZnO-host emission. The different maximum-peak positions of these bands stem from diverse types of growing techniques of ZnO materials (Table I). Variation of the emission intensities of the strongest RE^{3+}-ion transitions from Fig. 4 is shown in Fig. 5 as a function of temperature. We observed that the emissions of Pr^{3+} ($^3P_0 \rightarrow {}^3H_6$) and Tm^{3+} ($^1G_4 \rightarrow {}^3H_5$) ions quenched less with rising temperature than other investigated RE ions. However, even at 300 K, characteristic emission caused by 4f-4f shell transitions is clearly visible for all investigated RE ions.

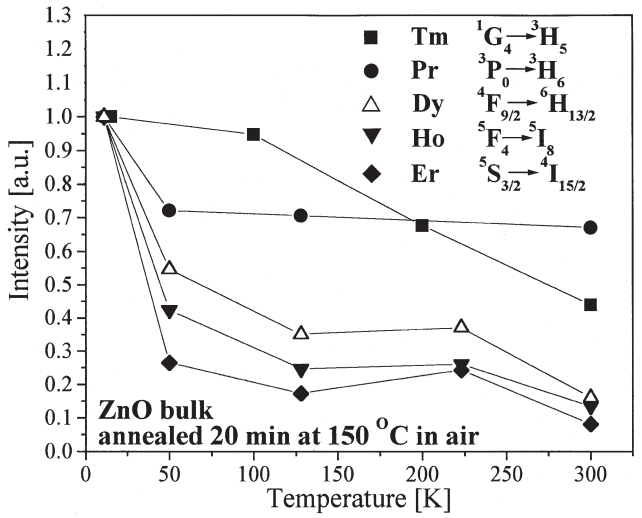

Fig. 5. The emission intensity (strongest transition lines from Fig. 1) of the RE ions implanted in bulk-ZnO single crystals normalized to unity and shown as a function of temperature.

LUMINESCENCE OF POLYCRYSTALLINE-SINTERED ZnO:RE^{3+} Li CO-DOPED PELLETS

First, it must be pointed out that the characteristic RE^{3+} emission from ZnO pellets doped with RE is observed under either direct or indirect (above bandgap) excitation only in the presence of coactivators ions (Li^+, Cl^-, or N^-). The luminescence spectra of ZnO:Nd:Li obtained under above-bandgap excitation and presented in Fig. 6a are similar to that reported by others.[13] They show the broad-band luminescence around 600 nm attributed to the ZnO host, with clearly visible, sharp, deep reabsorption peaks of the Nd^{3+} ions and a group of sharp lines around 910 nm caused by the $^4F_{3/2} \rightarrow {}^4I_{9/2}$ transition. Figure 6b shows the PL excitation (PLE) spectrum monitored at 904 nm for the $^4F_{3/2} \rightarrow {}^4I_{9/2}$ transition of the Nd^{3+} ion. A set of sharp lines detected in the PLE spectrum corresponds to the sharp, deep reabsorption peaks of the Nd^{3+} ions shown in spectrum (a). In addition, the spectra obtained by direct excitation of ZnO:Nd,Li pellets at 488 nm and 514 nm are also shown in Fig. 7.

The above-bandgap excitation (325 nm) of the ZnO:Dy,Li-sintered pellet results in the luminescence spectra shown in Fig. 8a. Several groups of transition lines from the $^4F_{9/2}$ level toward ^6H_J (J = 15/2, 13/2, 9/2) ground multiplets with a dominant one at 580 nm ($^4F_{9/2} \rightarrow {}^6H_{13/2}$) at 10 K were observed. It is seen that, with increasing temperature, the broad-ZnO luminescence at 540 nm is shifted to shorter wavelength, and the Dy^{3+} emission is quenched. At 300 K, only peaks at 504 nm ($^4F_{9/2} \rightarrow {}^6H_{15/2}$) and 650 nm ($^4F_{9/2} \rightarrow {}^6H_{11/2}$) survived. The PLE spectrum monitored at 579 nm (for the $^4F_{9/2} \rightarrow {}^6H_{15/2}$ Dy^{3+} transition) (Fig. 8a) shows that Dy ions are effectively excited in the above-bandgap excitation process

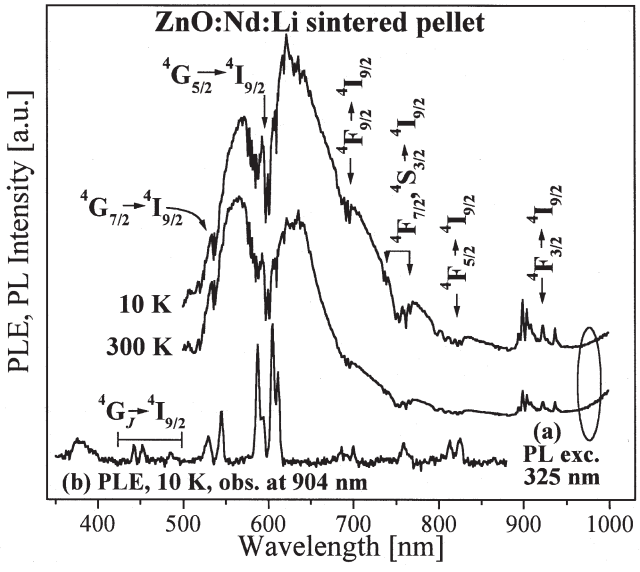

Fig. 6. The spectra of Nd^{3+} and Li^+-doped ZnO pellet: (a) PL excited by He-Cd (325 nm) measured at 10 K and 300 K and (b) PLE monitored at 904 nm and measured at 10 K.

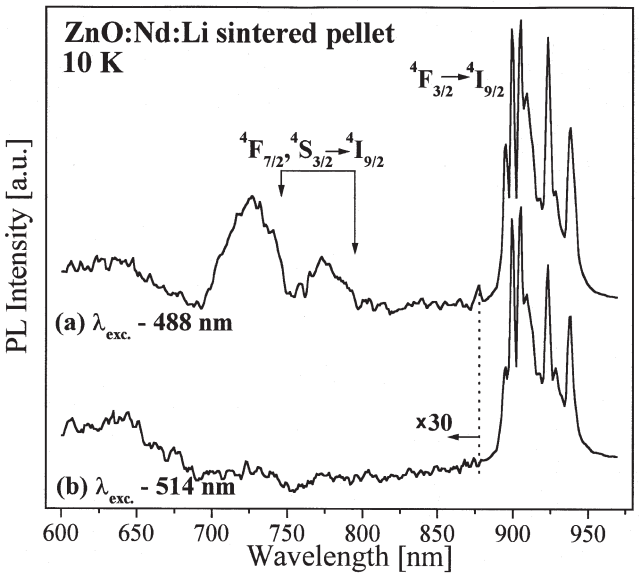

Fig. 7. The PL spectra of ZnO:Nd:Li-sintered pellet observed at 10 K for below-bandgap excitation with wavelengths of (a) 488 nm and (b) 515 nm.

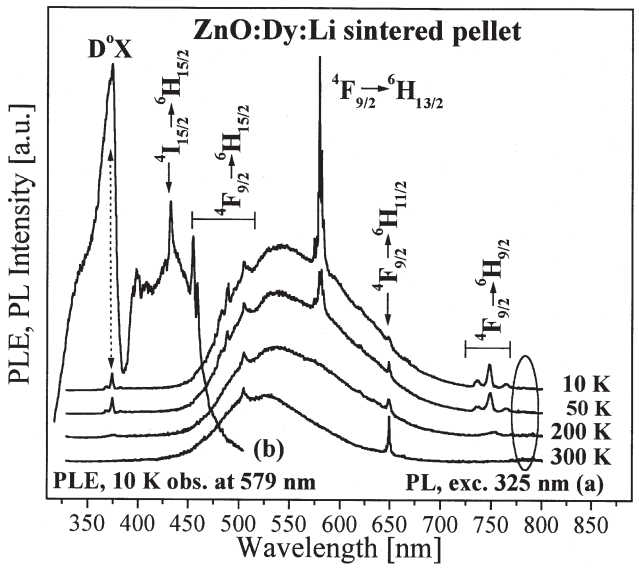

Fig. 8. The spectra of Dy^{3+} and Li^+-doped ZnO pellet: (a) PL excited by He-Cd (325 nm) measured at temperature from 10–300 K and (b) PLE monitored at 579 nm and measured at 10 K.

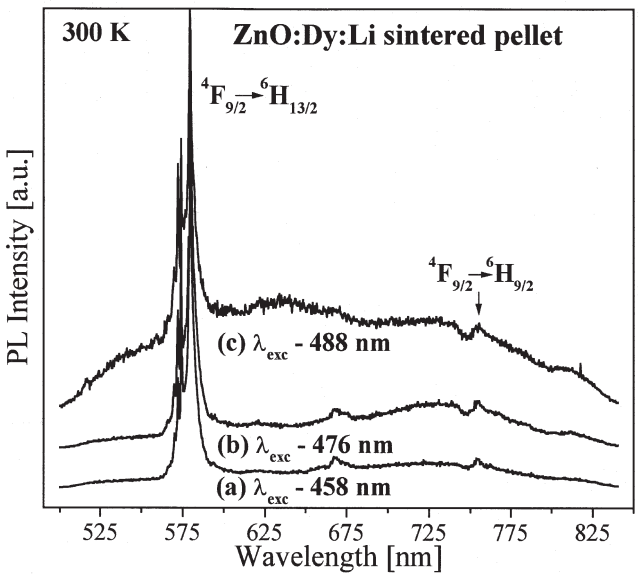

Fig. 9. The PL spectra of ZnO:Dy:Li-sintered pellet observed at 300 K for below-bandgap excitation with wavelengths of (a) 457 nm, (b) 476 nm, and (c) 488 nm.

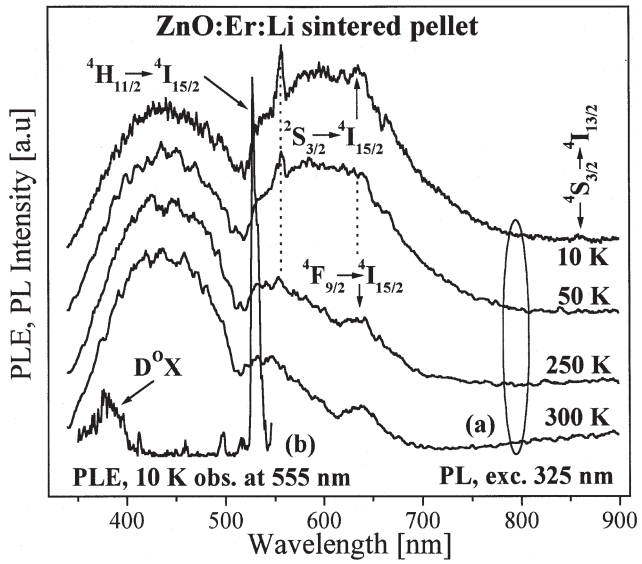

Fig. 10. The spectra of Er^{3+} and Li^+-doped ZnO pellet: (a) PL excited by He-Cd (325 nm) measured at temperature from 10–300 K and (b) PLE monitored at 555 nm and measured at 10 K.

through the energy transfer between the ZnO host and the RE centers. The luminescence spectra of ZnO:Dy:Li pellets obtained by direct excitation of Dy^{3+} ion in its $^4F_{9/2}$ level are shown in Fig. 9.

Figure 10a and b shows the (a) PL and (b) PLE spectra of the Er-doped ZnO:Li pellet. The emission spectra under the above-bandgap excitation, recorded in the temperature range 10–300 K, show the broad pattern of ZnO and two peaks at 556 nm and 860 nm attributed to $^2S_{3/2} \rightarrow {}^4I_J$ (J = 15/2, 13/2) transitions, detected only at low temperatures. Above 250 K, a new broad peak at 636 nm appears and can be assigned to the $^4F_{9/2} \rightarrow {}^4I_{15/2}$ transition. We believe that the dip at ~517 nm is due to a partial reabsorption of ZnO emission by the Er^{3+} ions. This conclusion is supported by the PLE spectrum monitored at 555 nm (transition $^2S_{3/2} \rightarrow {}^4I_{15/2}$), shown in Fig. 10b, which reveals a strong excitation peak assigned to the $^4H_{11/2} \rightarrow {}^4I_{15/2}$ transition and several smaller excitation lines in this spectral region attributed to the Er^{3+} ion. The luminescence spectra (Fig. 11) obtained by a direct excitation of the Er^{3+} ion at 458 nm, 496 nm, and 514 nm show several groups of transition lines without broad-ZnO emission, except the band at 760 nm with an uncertain origin.

Once again, the luminescence spectra of the ZnO:Tm:Li pellet obtained under the above-

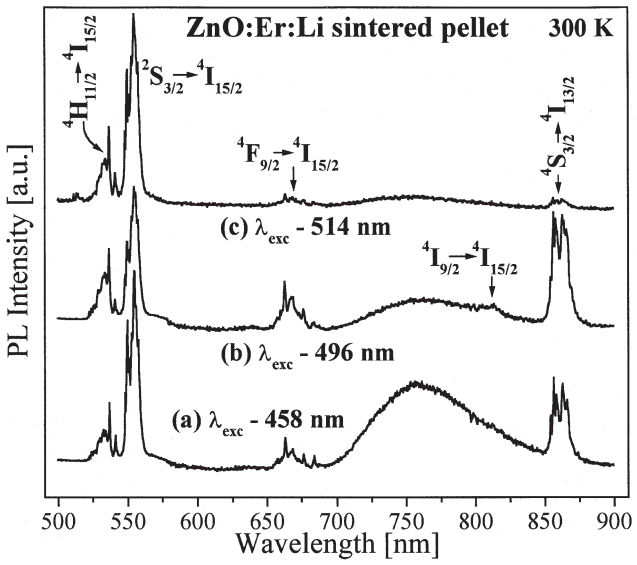

Fig. 11. The PL spectra of ZnO:Er:Li-sintered pellet observed at 300 K for below-bandgap excitation with wavelengths of (a) 458 nm, (b) 496 nm, and (c) 515 nm.

bandgap excitation (325 nm) are identical to that reported in the literature.[13] Figure 12a and b show (a) two PL spectra recorded at 10 K and 300 K and (b) the PLE spectrum monitored at 800 nm (transition $^1G_4 \rightarrow {}^3H_5$) recorded at 10 K. It is seen that the PL spectra exhibit the broad band around 640 nm of the ZnO host and dip at ~660 nm and ~690 nm because of a partial reabsorption of ZnO emission by the Tm^{3+} ions. The sharp lines around 800 nm are attributed to the $^1G_4 \rightarrow {}^3H_5$ transition. The PLE spectrum (Fig. 12b) shows groups of lines around 375 nm corresponding to the excitonic emission of ZnO and at 475 nm and ~685 nm caused by the excitation transitions of $^1G_4$, ^3F_J (J = 2, 3) levels of the Tm^{3+}

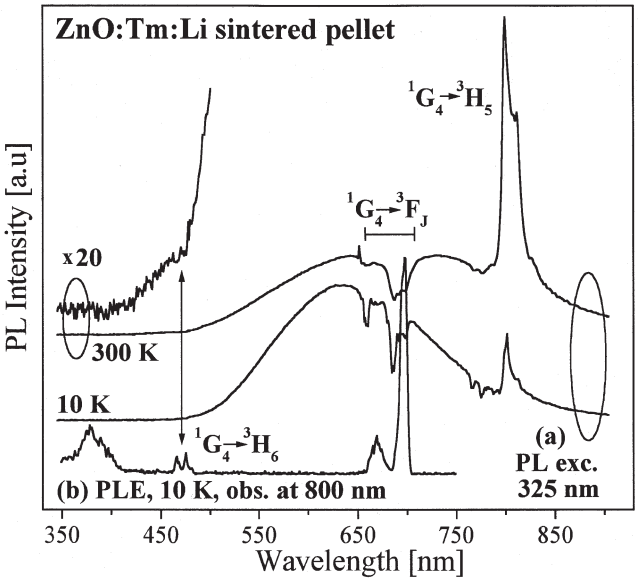

Fig. 12. The spectra of Tm^{3+} and Li^+-doped ZnO pellet: (a) PL excited by He-Cd (325 nm) measured at temperature 10 K and 300 K and (b) PLE monitored at 800 nm and measured at 10 K.

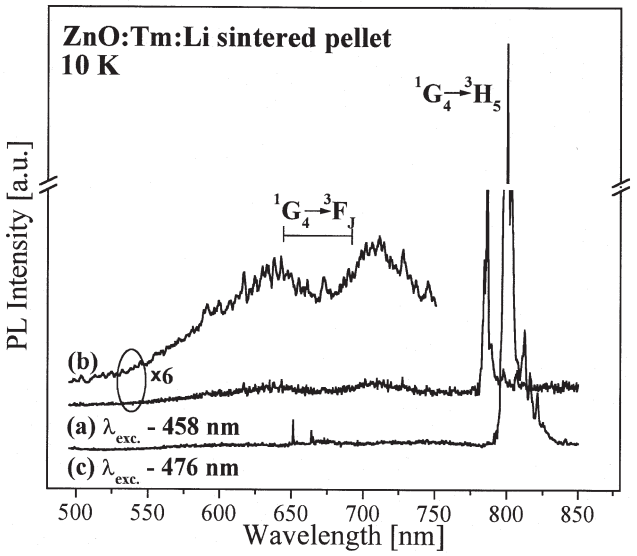

Fig. 13. The PL spectra of ZnO:Tm:Li-sintered pellet observed at 10 K for below-bandgap excitation with wavelengths of (a) 458 nm and (b) 476 nm.

ions, respectively. The luminescence spectra obtained by direct excitation of the $^1G_4$ level around 475 nm with laser wavelength at 458 nm and 476 nm are shown in Fig. 13. Both spectra show the weak broad bands peaking at ~640 nm and ~700 nm and strong line structure at 800 nm.

LUMINESCENCE OF POLYCRYSTALLINE-SINTERED ZnO:Tm:Cl AND ZnO:Eu:N PELLETS

The purpose of this study was to demonstrate that nitrogen and chlorine ions intentionally incorporated into RE-doped ZnO powder can act as RE-ion luminescence-coactivator agents. Figure 14 shows a

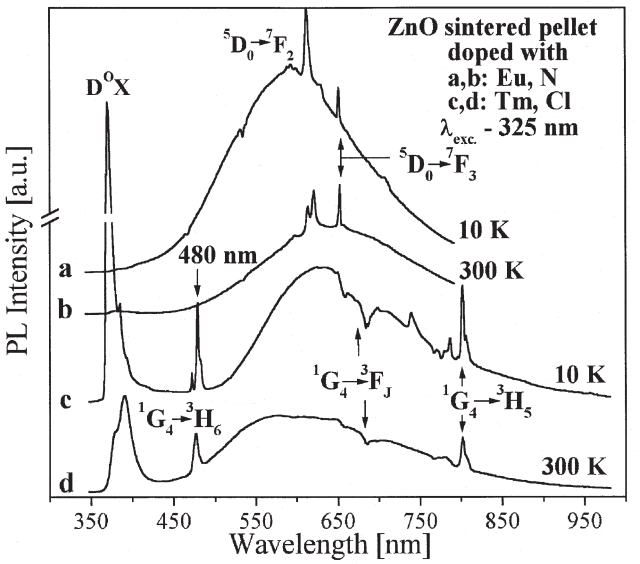

Fig. 14. (a) and (b) The luminescence spectra of sintered-ZnO:Eu:N pellet and sintered ZnO:Tm:Cl pellet and (c) and (d) samples excited with wavelength of 325 nm at 10 K and 300 K.

set of PL spectra recorded for two different types of phosphors: (a) and (b) ZnO:Eu,N and (c) and (d) ZnO:Tm,Cl. Spectra were recorded at 10 K and 300 K using a He-Cd laser (325 nm) as the above-bandgap excitation source. The PL spectra of ZnO:Eu,N pellets in Fig. 14a and b show characteristic Eu^{3+} emission because of the $^5D_0 \rightarrow {}^7F_J$ (J = 2, 3) transitions overlapped with the ZnO SA-emission band and are very similar to those published in other reports.[18] Figure 14c and d present spectra of ZnO:Tm,Cl pellets sintered at 1,100°C in a vacuum. Two significant features have been observed. The first one is the strong excitonic emission around 375 nm, and the second, which has not been observed before,[11] the blue emission lines assigned to the $^1G_4 \rightarrow {}^3H_6$ transition observed at 10 K and room temperature. The spectra are similar to the spectra of ZnO:Tm,Li shown in Fig. 12a except that the blue emission ($^1G_4 \rightarrow {}^3H_6$) for sample ZnO:Tm,Li is merely detectable.

DISCUSSION AND CONCLUSIONS

The early attempts of doping polycrystalline ZnO with RE were disappointing because no characteristic RE^{3+} narrow-line emissions had been found, only the broad structureless-band emission around 2.25 eV, attributed mistakenly to transitions between RE^{3+} donor and V_{Zn} acceptor pairs.[9] The first characteristic 4f emission was obtained from polycrystalline ZnO doped with RE (Pr^{3+}, Sm^{3+}, Eu^{3+}, Ho^{3+}, Er^{3+}, and Tm^{3+})[10] and co-doped with Li and from ZnO:Eu,N.[18] The PL, EL, and CL of sintered polycrystalline-ZnO pellets doped with RE^{3+} ions (Nd^{3+}, Sm^{3+}, Eu^{3+}, Dy^{3+}, Ho^{3+}, Er^{3+}, and Tm^{3+}) and co-doped with Li^+ have been also investigated.[12–14] In the latest paper, the UV excitation at 390 nm (3.179 eV below bandgap) for the same RE ions (Sm^{3+}, Eu^{3+}, Dy^{3+}, and Tm^{3+}) shows 4f emission in addition to the green SA ZnO broad-band spectra. The Nd^{3+}-, Dy^{3+}-, Ho^{3+}-, and Er^{3+}-doped samples under 365 nm (3.397 eV) excitation exhibit only the SA luminescence of the ZnO host with a partial reabsorption of the emitted SA band by the RE^{3+} ions. The PL of Tm^{3+} obtained by band-to-band excitation show only emission at ~800 nm.[10–14] The x-ray analysis and scanning electron microscopy indicated that the RE^{3+} ions are closely associated with Li^+ ions and are mainly located at the grain boundaries of the polycrystalline-ZnO pellets. The polycrystalline-ZnO samples, doped with Eu_2O_3 or $EuCl_3$ baked in dry air at 1,100°C for 3 h, show weak line emission of Eu^{3+} ions ($^5D_0 \rightarrow 7_{F_2}$ transition) observed on a broad band of host luminescence at room temperature.[15] Recently, pure-red-emitting phosphor was synthesized using ZnO:$EuCl_3$ pellets sintered at 1,100°C in a vacuum.[16,17] This was the first successful attempt that demonstrated that the SA band at 530 nm can be completely suppressed in the PL emission spectrum. It suggests that the energy from generated electron-hole pairs is efficiently transferred to the Eu^{3+} ions, giving rise to sharp, red emission peaks at 620 nm and attributed to transitions ^5D_J (J = 0,1) $\rightarrow {}^7F_J$ (J = 0,1,6) of Eu^{3+} ions. Under the electron excitation, the relative brightness of the red emission from ZnO:Eu,Cl is about 15% of green CL for undoped ZnO. The analysis of x-ray diffraction and PL spectra measurements indicate that, for ZnO:$EuCl_3$ phosphors sintered in vacuum, Eu exists in the ZnO lattice as the tetragonal phase of EuOCl and effectively transfers energy to 4f electrons of the Eu^{3+} ion, eliminating the broad-band emission of the ZnO host. These results, together with x-ray diffraction, PLE spectra, and time-resolved spectra measurements, suggest that an energy-transfer process occurs from the ZnO host to the Eu^{3+} ion, which exists in the host lattice in the form of EuOCl.

The ZnO:Er thin films fabricated by laser ablation were investigated using PL spectroscopy and their kinetics under different excitation conditions, where Er ions are either indirectly excited by the electron-hole-mediated process from a ZnO host or directly excited to selected energy states of Er^{3+} ions.[21–24] Photoluminescence peaking at 378 nm caused by the ZnO host was observed in ZnO:Er films under over-bandgap excitation (325 nm), together with Er-related PL only in the infrared region at around 1.54 μm. There is no change in the Er^{3+} 1.54-μm emission spectrum for the different excitation conditions, whereas dramatic change is seen in the rise time of the 1.54-μm emission. The rise time of the 1.54-μm emission observed for indirect excitation (above bandgap of ZnO) was shorter than for direct excitation of Er^{3+}ions. This fact is significant for light-emitting diode applications where the electron-hole pairs can be generated by the current injection in p-n junction and excite the Er^{3+} ions. The direct photoexcitation of Er^{3+} ions to the $^2H_{11/2}$ level by the 526-nm excitation once relaxed to the $^4S_{3/2}$ level just below, induces the 1.54-μm emission as the last step of a cascaded de-excitation process of $^2H_{11/2} \rightarrow {}^4S_{3/2} \rightarrow {}^4I_{13/2} \rightarrow {}^4I_{15/2}$ transitions. The local structure of an optically active center in erbium-doped zinc-oxide (ZnO:Er) thin film produced by a laser-ablation technique was investigated by Er LIII-edge, x-ray absorption fine structure (XAFS) analysis using a synchrotron radiation as an x-ray source.[23] After ZnO:Er film deposition by laser ablation at 300 K, the sample was annealed in an oxygen atmosphere at 700°C for 3 min for the activation of Er^{3+} ions.

The PL intensity at 1.54 μm of the annealed sample was about 500 times stronger than that of as-deposited thin film. The XAFS measurements carried out for the as-ablated film and the annealed one reveal that in as-ablated ZnO:Er thin film, Er has an approximately fivefold coordination of O surrounded by eight other O atoms as second-nearest neighbors. After annealing in O_2 ambient, the local structure of Er changes to a pseudo-octahedral structure with C_{4v} symmetry, similar to the optically activated Er-doped Si (Si:Er),[24] resulting in strong PL. Authors[24] believe that the high-order coordination of O

decreases the Er-related (PL) intensity because of an undesirable crystal field for 4f-4f radiative transition. From the preceding review, it is difficult to derive general conclusions about the nature of the RE-luminescent center in ZnO. Most of the research was performed on polycrystalline samples where the crystalline boundary can play a dominant role in the structure of the RE-luminescent center. The ionic radii for all RE^{3+} ions are bigger than the radius of Zn^{2+}. They are in the range of 1.02 Å for Ce^{3+} to 0.94 Å for Yb^{3+}, while the radius of $Zn^{2+}$is only 0.74 Å. Incorporation of trivalent RE ions into ZnO causes a big distortion in the ZnO crystal lattice (solubility of RE in ZnO is low) and also requires association with other charge-compensating lattice defects or impurities nearby.[25] The electron-spin resonance studies of ZnO doped by diffusion with Yb reveals two sites of Yb^{3+} ions substitutional for Zn^{2+} ions and an interstitial site.[26]

The investigation presented in this paper was performed on the ZnO-bulk and thin-film single crystal and is the first report of the visible emission from RE ions (Pr^{3+}, Sm^{3+}, Dy^{3+}, Ho^{3+}, and Tm^{3+}) incorporated into ZnO single crystal. We also study the sintered polycrystalline-ZnO:RE pellets, codoped with Li, Cl, and N. Experiments show that the characteristic RE^{3+} emission from ZnO pellets doped with RE is observed under either direct or indirect (above bandgap) excitation only in the presence of coactivator ions (Li^+, Cl^-, or N^-). For ZnO:Tm,Cl pellets, two significant features have been observed. The first one is the strong excitonic emission around 375 nm. The second one is the not-reported-before[11] blue emission lines assigned to the $^1G_4 \rightarrow {}^3H_6$ transition, observed in the temperature range of 10–300 K. The spectra are similar to the spectra of ZnO:Tm,Li except that the blue emission for sample ZnO:Tm,Li is merely detectable.

The isochronal-annealing experiment in the temperature range of 25–1,100°C of ZnO:RE,Li bulk crystals and epilayers shows that annealing at 150°C brought up RE emissions approximately two times stronger than recorded for as-implanted (unannealed) samples. Still further annealing at temperatures above 150°C revealed that the characteristic sharp-line emission spectra of RE ions became less resolved and gradually disappeared when annealing temperature approaches 300°C. The deactivation energy estimated from the annealing dependence of RE line-emission intensity is 0.27 eV, which is comparable to the energy required for zinc-interstitial motion.[20] Annealing the samples above 300°C up to 1,100°C does not recover RE emissions. Both types of samples show RE-characteristic emission only under CL excitation, with the exception of the Tm-doped bulk crystal, which shows Tm^{3+}-emission lines (at ~800 nm) excited by photons above bandgap (PL) and by electrons in CL.

Figure 15a and b shows a model of the excitation processes for ZnO doped with RE ions. It is assumed that the indirect excitation of RE ions in ZnO proceeds through the nonradiative transfer of energy from the exciton bound to the RE-complex (REC) trap (intermediate REC-trap, Fig. 15b), which contains RE ions and native defects (and/or impurities) required for charge compensation in ZnO host. The energy overlap between the broad-band emission and RE-energy levels does not guarantee energy transfer because the local environment around the RE ion plays a significant part in the transfer process so that any one RE configuration may only couple to selected bands. Also, if the collapsing energy of an exciton bound to such a complex center is not sufficient to excite the 4f shell of the RE^{3+} ion (Fig. 15a, E_1 for REC-trap or E_2 and E_3 for other mediating centers[25]), the characteristic 4f emission of the RE ion will be not present. For some ions, the lowest 4f-energy levels are excited, and only infrared emission is observed. In the case of CL, excitation occurs through both direct impact excitations of RE ions by hot electrons or indirectly by generation electron-hole pairs and transfer energy to the 4f shell via the mechanism discussed previously. The absence of characteristic emission by RE^{3+} ions in CL of bulk ZnO and epilayer samples annealed above 300°C is due to the thermal creation of a local structure with an undesirable crystal field for 4f-4f radiative transitions. The energy-transfer rate can

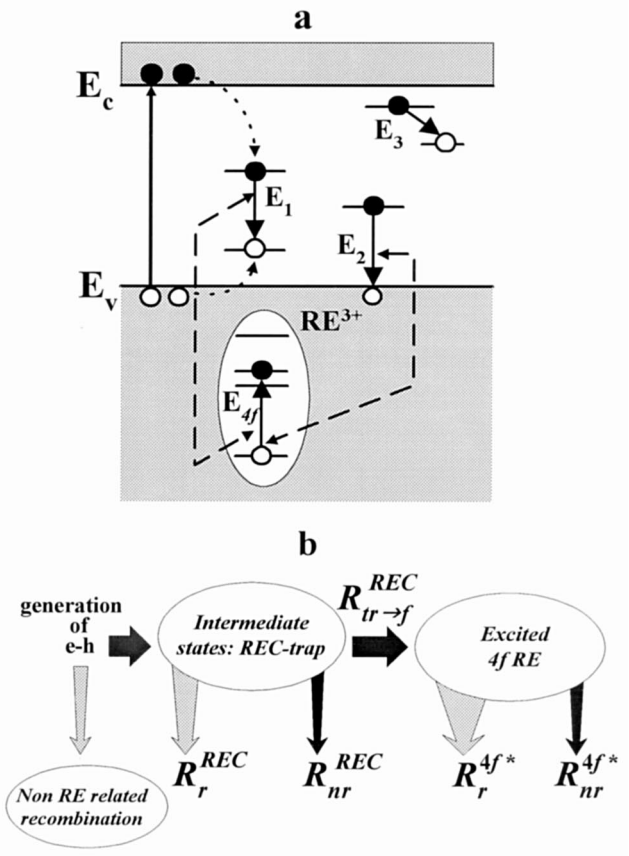

Fig. 15. The model of indirect-excitation process of RE ions in ZnO samples: (a) band diagram and (b) schematic of nonradiative transfer of energy from a generated electron-hole pair to REC-trap. All symbols are explained in the text.

be discussed for a simplified system in Fig. 15a, consisting of an intermediate REC-trap, and an RE^{3+}-$4f^n$ electron system. The symbols R_r^{REC}, R_{nr}^{REC}, and R_{tr-f}^{REC} are the radiative and nonradiative recombination rate of exciton on REC-trap, and energy transfer rate to RE-$4f^n$ electrons, respectively. The R_r^{4f*} and R_{nr}^{4f*} are the radiative and nonradiative recombination rates of the excited RE^{3+} ion. Assuming that there is no back transfer of energy from $4f^n$ electrons (justified by the long RE^{3+} decay time it) and that the transfer rate R_{tr-f}^{REC}, is much higher than R_r^{REC}, the SA broad-band emission will be suppressed or completely vanish. This model explained the Eu emission in the ZnO:$EuCl_3$ phosphor,[16,17] where the Eu exists in the ZnO lattice as the tetragonal phase of EuOCl and effectively transfers energy to 4f electrons of Eu^{3+} ion, eliminating the broad-band emission of the ZnO host. We believe that a similar center, TmOCl, with tetragonal phase is responsible for the PL emission of Tm^{3+}shown in Fig. 14c and d.

We also observed the radiative energy transfer in ZnO:RE,Li-sintered pellets. The SA band emission overlaps the absorption of the RE ion. In such a process, the shape of the SA band is modified by the absorption lines of the RE ion. The efficiency of energy transfer depends on the sample geometry and scattering processes. The lifetime of the SA luminescence is unaffected, and there is no correlation between the SA emission and following absorption by the RE ion. The big difference in luminescence between single-crystal and polycrystalline ZnO doped with RE is due to a grain boundary. The grain boundaries in polycrystalline ZnO have received much attention because they are considered to be the origin of the material nonlinear I-V characteristic, and it is believed that the RE-luminescence centers are localized at a grain boundaries.[11–14,27]

ACKNOWLEDGEMENTS

The authors acknowledge the support of the NSF through Grant No. ECS-0083412 and the O.U. Stocker Fund. The authors thank Cermet, Inc. for providing the ZnO-bulk samples used for this study. We express our gratitude to Dr S. Kaya, School of EECS, OU, for critical reading of this manuscript.

REFERENCES

1. M. Kasuga and S. Ogawa, *Jpn. J. Appl. Phys.* 22, 749 (1983).
2. Y. Sato and S. Sato, *Thin Solid Films* 281–282, 445 (1996).
3. M. Joseph, H. Tabata, and T. Kawai, *Jpn. J. Appl. Phys.* 38, L1205 (1999).
4. K. Winegish, Y. Koiwai, Y. Kikuchi, K. Yano, M. Kasuga, and A. Shimizu, *Jpn. J. Appl. Phys.* 36, L1453 (1997).
5. X.L. Guo, H. Tabata, and T. Kawai, *J. Cryst. Growth* 223, 135 (2001).
6. D.C. Reynolds, D.C. Look, B. Jogai, C.W. Litton, T.C. Collins, W. Harsch, and G. Cantwell, *Phys Rev. B* 57, 12151 (1998).
7. D.C. Reynolds, D.C. Look, and B. Jogai, *J. Appl. Phys.* 89, 6189 (2001) and references therein.
8. (a) B.J. Pierce and R.L. Hengehold, *J. Appl. Phys.* 47, 644 (1976). (b) J.A. Garcia, A. Remon, and J. Piqueras, *J. Appl. Phys.* 62, 3058 (1987).
9. S. Bhushan, B.R. Kaza, and A.N. Pandy, *Pramana* 11, 67 (1978) and references therein.
10. K. Kynev and V.K. Kuk, *Dokl. Bolg. Akad. Nauk* 41, 61 (1988).
11. J.C. Ronfard-Haret and J. Kossanyi, *Chem. Phys.* 241, 339 (1999).
12. J. Kossanyi, D. Kouyate, J. Pouliquen, J.C. Ronfard-Haret, P. Valat, D. Oelkrug, U. Mammel, G.P. Kelly, and F. Wilkinson, *J. Lumin.* 46, 17 (1990).
13. S. Bachir, K. Azuma, J. Kossanyi, P. Valat, and J.C. Ronfard-Haret, *J. Lumin.* 75, 35 (1997) and references therein.
14. J.C. Ronfard-Haret, J. Kossanyi, and J.L. Pastol, *J. Phys. Chem. Solids* 62, 565 (2001).
15. Y. Hayashi, H. Narahara, T. Uchida, T. Noguchi, and S. Ibuki, *Jpn. J. Appl. Phys.* 34, 1878 (1995).
16. Y.-K. Park, J.-I. Han, M.-G. Kwak, H. Yang, S.-H. Ju, and W.-S. Cho, *Appl. Phys. Lett.* 72, 668 (1998).
17. Y.-K. Park, J.-I. Han, M.-G. Kwak, H. Yang, S.-H. Ju, and W.-S. Cho, *J. Lumin.* 78, 87 (1998).
18. V.Q. Quang, N.Q. Liem, N.C. Thanh, T.V. Chuong, and L.T.L. Thanh, *Phys. Status Solidi (a)* 78, K161 (1983).
19. H.J. Lozykowski, W.M. Jadwisienczak, and I. Brown *J. Appl. Phys.* 88, 210 (2000).
20. F.J. Bryant, *Prog. Cryst. Growth Charact.* 6, 191 (1983).
21. S. Komuro, T. Katsumata, T. Morikawa, X. Zhao, H. Isshiki, and Y. Aoyagi, *Appl. Phys. Lett.* 76, 3639 (2000).
22. X. Zhao, S. Komuro, H. Isshiki, Y. Aoyagi, and T. Sugano, *J. Lumin.* 87–89, 1254 (2000).
23. M. Ishii, S. Komuro, T. Morikawa, and Y. Aoyagi, *J. Appl. Phys.* 89, 3679 (2001).
24. M. Ishii, T. Ishikawa, T. Ueki, S. Komuro, T. Morikawa, Y. Aoyagi, and H. Oyanagi, *J. Appl. Phys.* 85, 4024 (1999).
25. H.J. Lozykowski, *Phys.Rev. B* 48, 17758 (1993).
26. P. Schreiber and A. Hausmann, *Solid State Commun.* 8, 1103 (1970).
27. J.M. Carlsson, B. Hellsing, H.S. Domingos, and P.D. Bristowe, *J. Phys.: Condens. Matter* 13, 9937 (2001) and references therein.